

## Effect of Heat Input on Mechanical and Metallurgical Properties of Gas Tungsten Arc Welded Lean Super Martensitic Stainless Steel

Chellappan Muthusamy<sup>a</sup>, Lingadurai Karupiah<sup>b</sup>, Sathiya Paulraj<sup>c\*</sup>,

Devakumaran Kandasami<sup>d</sup>, Raja Kandhasamy<sup>b</sup>

<sup>a</sup>Department of Mechanical Engineering, Dhanalakshmi Srinivasan Engineering College, Perambalur-621212, Tamilnadu, India.

<sup>b</sup>Department of Mechanical Engineering, University College of Engineering, Anna University, Dindigul-624622, Tamilnadu, India.

<sup>c</sup>Department of Production Engineering, National Institute of Technology, Tiruchirappalli-620015, Tamilnadu, India

<sup>d</sup>Welding Research Institute, BHEL, Tiruchirappalli, Tamilnadu, India

Received: September 10, 2015; Revised: January 14, 2016; Accepted: March 7, 2016

Welding of 6mm thick AISI: 410S lean super martensitic stainless steel (LSMSS) under different heat input of 7.97, 8.75 and 10.9 kJ/cm was carried out by gas tungsten arc welding process. The influence of heat input on metallurgical and mechanical properties in weld and HAZ region was studied. The tensile tests were carried out at different temperatures, namely at room temperature, at 600°C, 700°C and 800°C. It is observed that rise in the heat input and temperature decreased the tensile strength of the weld joint. Further it is noticed that rise in the heat input enhanced the toughness of weld deposit but hardness of weld joints showed insignificant variation in it. This was primarily due to the increase in ferrite content in the matrix of martensite by enhancement of the heat input. In general, the microstructures of weld consisted of mixture of martensite and austenite as well as some amount of ferrite. Whereas, HAZ near to the fusion line consisted of larger and more elongated bright phase of banded delta ferrite in a matrix of martensite irrespective of change in heat input.

**Keywords:** Heat input, Lean super martensitic stainless steel, Microstructure, Mechanical properties, Fracture surface

## INTRODUCTION

Lean super martensitic stainless steel (LSMSS) is a better alternative to high-strength low-alloy (HSLA) steel. It is mostly used in oil and gas industry<sup>1</sup>. The LSMSS is developed from classic martensitic stainless steel (11–14% Cr) by reducing Carbon content and adding Nickel to enhance resistance to welding and weldability<sup>2</sup>. The superior property achieved in LSMSS is primarily due to the precipitation of Cr<sub>2</sub>N. In general, the microstructure of LSMSS consists of martensite and a variable amount of austenite (up to 30%) as well as ferrite (up to 10%) in varied form and structure<sup>3</sup>. In recent years, a lot of research work has been carried out on LSMSS related to the influence of different heat treatments on its welding. Some of the related literatures are discussed below.

Ma et al.,<sup>4</sup> reported that an addition of 0.1% Ni to 5%Ni in martensitic stainless steel improved the strength and reduced the ductility after tempering as a result of severe precipitation of Cr<sub>2</sub>N. Liu et al.,<sup>5</sup> investigated the mechanical and metallurgical properties of 13 Cr SMSS under different heat treatment processes. It was observed that after quenching, the material had lath martensites along with less amount of austenite<sup>6</sup>. Kumar et al.,<sup>7</sup> analyzed the

influence of preheating temperature on hardness of SMSS. It was concluded that samples preheated at 30° C had higher hardness value compared to the samples preheated at 120° C due to the faster cooling rate related with lesser preheat temperature. In the line of these findings, Zappa et al.,<sup>8</sup> also made a systematic approach to increase the weldmetal toughness of super martensitic stainless steel by modifying the microstructure and by means of different post weld heat treatments and shielding gas. It was observed that, the Ar-18%CO<sub>2</sub> shielding gas had less toughness and increased strength when compared to Ar-5%He shielding gas. The low toughness observed in case of Ar-5% He shielding gas was primarily due to the presence of un-tempered martensite in the weld deposit. Hence, it is well understood that the SMSS has high heat sensitivity and thus suitable welding processes and procedures are very much required.

Omura et al.,<sup>9</sup> reported that laser welded super martensitic steel had better corrosion resistance than ERW and GTAW welded super martensitic steel. The main reason for the improved corrosion resistance was the faster cooling of the weld metal without precipitation and segregation. Taban et al.,<sup>10</sup> inferred that the quality of weld joint with respect to the strength and toughness of SMSS improved by using plasma arc welding. Aquino et al.,<sup>11,12</sup> investigated the

\*e-mail: [psathiya@nitt.edu](mailto:psathiya@nitt.edu)

corrosion behavior of Electron beam welded super martensitic stainless steels under two conditions namely (i) matching consumables, and (ii) without matching consumables. In both cases, corrosion resistance improved due to rapid cooling of the weld metal. Based on these, it was concluded that, the high energy processes gave better properties of the SMSS weld joint. However, these high energy processes are not economical and versatile.

Della Rovere et al.,<sup>13,14</sup> studied the metallurgical and mechanical aspects of radial friction welded SMSS pipes in welded condition. The results showed that the tensile strength revealed higher weld strength than that of the base material tensile strength and it was also confirmed that the radial friction welding process could be applied to SMSS pipes. Bala Srinivasan et al.,<sup>15</sup> inferred that the SMSS welded by sub merged arc welding process was susceptible to embrittlement under hydrogen charging conditions.

Based on the literature, it is obvious that the welding of lean super martensitic stainless steel (LSMSS) by electric arc welding processes is critical. The criticality primarily starts from proper selection of welding parameters such as arc voltage (V), welding current (I) and travel speed (S) to post weld heat treatment. Moreover, the thermal influence of welding process on quality of weld deposit largely depends on heat input of the process. In case of arc welding, the heat input is the welding power ( $V \times I$ ) divided by the travel speed.

It is generally well known that increased heat input results in cracking of weld metal and Heat Affected Zone (HAZ). The cracking occurs due to adverse development of residual stress and unwanted metallurgical changes in the weldment. In addition, high heat input may introduce higher amount of  $\delta$  ferrite content<sup>16-18</sup> in the weld deposit which reduces the corrosion resistance and leads to premature failure during service. The superior mechanical properties can be achieved in the SMSS weld when the microstructure of weld and HAZ be properly tempered<sup>19</sup> which also depends on heat input of the process.

But, there was very limited visible literature on welding of LSMSS. Particularly arc welding of LSMSS is very limited. It is due to fast cooling rate which creates the brittle phase. It suppresses the strength of the joints.

At present, one of the major challenges facing for welding of LSMSS material is to achieve superior mechanical and metallurgical properties of weld joint which in turn provide a long life and fulfill service requirement conditions. Thus, special attention is required for optimal welding procedures for LSMSS and for the behaviour of weldments for different applications. It is well known that severity of weld thermal cycle produced by gas tungsten arc welding (GTAW) is comparatively less than other arc welding techniques. Hence, it is largely realized that use of GTAW may improve the properties of LSMSS weld joint. Thus, the present investigation focuses on the effect of heat inputs (7.97, 8.75 and 10.9 kJ/cm) on mechanical and metallurgical properties of LSMSS welds by GTAW process. This study may provide wider opportunity to extend the application of LSMSS for various industrial applications.

## 2. EXPERIMENTAL PROCEDURE:

### 2.1. Welding

The chemical compositions of LSMSS base and corresponding filler materials used for the present investigation are given in Table 1.

A 6 mm thick plate of LSMSS was welded by GTAW with multi-pass welding procedure using single V groove and DCEN polarity under 99.97% argon gas shielding at a flow rate of 15 lpm. The electrode used for the present investigation was 2% Thoriated tungsten electrode having a diameter of 2.4mm. Prior to welding the plates were cleaned to remove any oxide and faying surfaces. The welding parameters were selected based on the initial trials and the parameters were identified as given in Table 2.

During welding, preheat and inter pass temperatures were maintained at 100°C. In case of GTAW process, the heat input (HI) can be defined as a product of arc voltage (V) and welding current (I) divided by welding speed (S).

### 2.2. Studies on Mechanical and Metallurgical Properties of LSMSS weld joints

Prior to mechanical and metallurgical testing, the weld joints were subjected to radiography inspection to ensure the weld joint quality. Microstructure characterizations

**Table 1.** Chemical composition of base metal, filler wire and multi-pass GTA weld deposits

Material / Exp. No	Chemical Composition, Wt%										
	C	Si	Mn	P	S	Cr	Mo	Ni	Cu	Ti	Fe
Base metal	0.02	0.21	0.62	0.02	0.01	12.21	2.02	5.38	0.21	0.03	Bal
ER: 410 Filler Rod	0.12	0.42	0.68	0.02	0.02	12.10	--	--	--	--	Bal
Butt Joint-1	0.024	0.47	0.61	0.18	0.20	11.21	--	5.27	0.09	0.06	Bal
Butt Joint-2	0.022	0.56	0.64	0.19	0.11	11.17	--	5.21	0.12	0.09	Bal
Butt Joint-3	0.017	0.54	0.72	0.24	0.30	12.96	--	5.31	0.07	0.09	Bal

**Table 2.** Welding parameter used for present investigation

Weld Joint	Heat Input ( $V \times I$ ) / S, kJ/cm	Welding Parameters		
		Welding Current, I	Arc Voltage, V	Welding Speed, cm/min
Butt Joint -1	7.97	100	11.3	8.5
Butt Joint -2	8.75	120	10.7	8.8
Butt Joint -3	10.9	140	11.2	8.6

were carried out at different weld zones with the help of Optical Microscope (OM). The chemical composition of the multi-pass weld deposits were measured using Scanning Electron Microscope (SEM) with Energy Dispersive X-ray Analysis (EDAX) techniques. The chemical composition of weld deposits were measured at the center of the weld ensuring the dilution of base metal was not extended to the weld center. The sample was prepared as per metallographic techniques and etched with 5ml Vilella's reagent, 5ml HCl, 1gsm picric acid and remaining methanol by using electrolytic procedure. Fischer ferritoscope was used to find out the percentage of ferrite phases in the different regions of weld zones. The precipitation behavior was studied by XRD. Micro-hardness measurements were taken on the LSMSS weldment across the transverse direction using micro Vickers hardness tester as per ASTM E370 standard. The tensile tests of weld joints were carried out under different temperatures: at room temperature (RT), at 600°C, 700°C and 800°C. The tests were carried out as per the ASTM: E8 standard. Three samples were tested to ensure the reliability of the experiment and the average value was reported. After that, the fracture surfaces of the tensile samples were analyzed using SEM. Room temperature Charpy V-notch test was conducted from the transverse cross-section of weldments as per ASTM E-23 standard.

### 3. RESULTS AND DISCUSSION

#### 3.1 Soundness of Weld Joint

Typical macrograph of LSMSS weld joints made by GTAW process under different heat input of 7.97, 8.75 and 10.9 kJ/cm are shown in Figure 1 (a-c).

From the Figure 1 (a-c) it is observed that, the weld joints had proper fusion without any defects. Further it is noticed that rise in heat input also enhanced the area of weld metal which might influence the microstructure of weld joint.

#### 3.2 Metallurgical properties

The microstructure of AISI: 410S base metal is shown in Figure 2 (a & b).

The microstructure of the base metal consisted of a mixture of martensite and ferrite along with banded rolled structure. In the mapping image it is clearly noted that the ferrite content in the martensitic phase was around 46%. The measured chemical compositions of multi-pass GTA weld deposit under different heat input are given in Table 2. It is observed that the chemistry of weld deposit varied with the change in heat input and accordingly influenced the microstructure of weld joints.

Typical change in microstructure of weld deposit prepared under different heat inputs of GTAW process are shown in Figure 3 (a-c). Figure 3 (a) depicts that at low heat input the microstructure of weld deposit consisted of bright phase of  $\delta$ - ferrite in the martensitic matrix (dark) whereas an increase in heat input (Figure 3 (b)) changed the shape of the  $\delta$ - ferrite to plate shape. At higher heat input (Figure 3 (c)), the microstructure of weld deposit consisted of a similar feature as observed in case of low heat input weld deposits.

However, the shape of the  $\delta$ - ferrite was feathery in nature and the dendritic grain size was coarser than those of the low heat input weld deposits. This was in agreement with the earlier study reported in case of Gleeble simulation study of SMSS on various mechanical and metallurgical properties of weld joint. The results showed that superior mechanical and metallurgical properties were achieved when the grain size was small and the volume fraction of  $\delta$  ferrite content was uniformly distributed in the matrix<sup>20</sup>. In the line of these observations, the measured  $\delta$  ferrite content in the weld deposits produced under different heat input of GTAW process are given in Table 3.

It is observed that an increase in heat input enhanced the  $\delta$ - ferrite in the matrix due to higher solidification rate. This behavior largely reflected in the weld microstructure as explained earlier (Figure 3 (a-c)). The HAZ represents

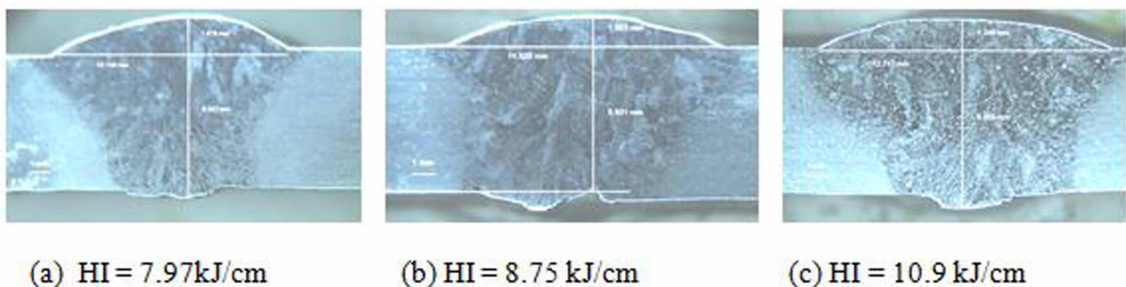


Figure 1. Macrograph of GTAW weld joints

Table 3. Measured  $\delta$  ferrite content in the weld deposits

Exp. No.	Heat Input, kJ/cm	Weld metal		HAZ	
		% of Martensite	% of ferrite	% of martensite	% of ferrite
Butt joint-1	7.97	63	37	69.66	31.22
Butt joint-2	8.75	59.17	41.49	70	30
Butt joint-3	10.9	57	43	88.60	11.78

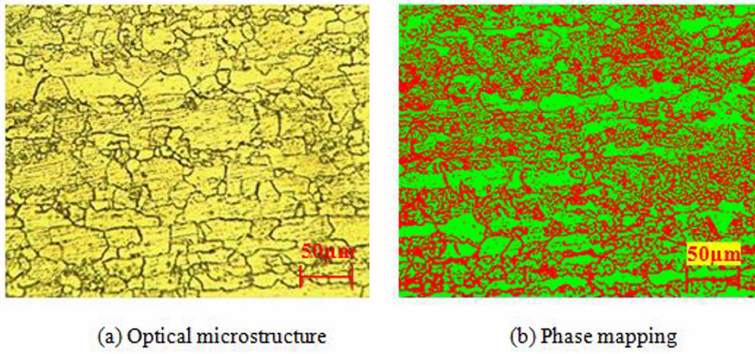


Figure 2. (a & b) Typical microstructure of AISI:410S base metal

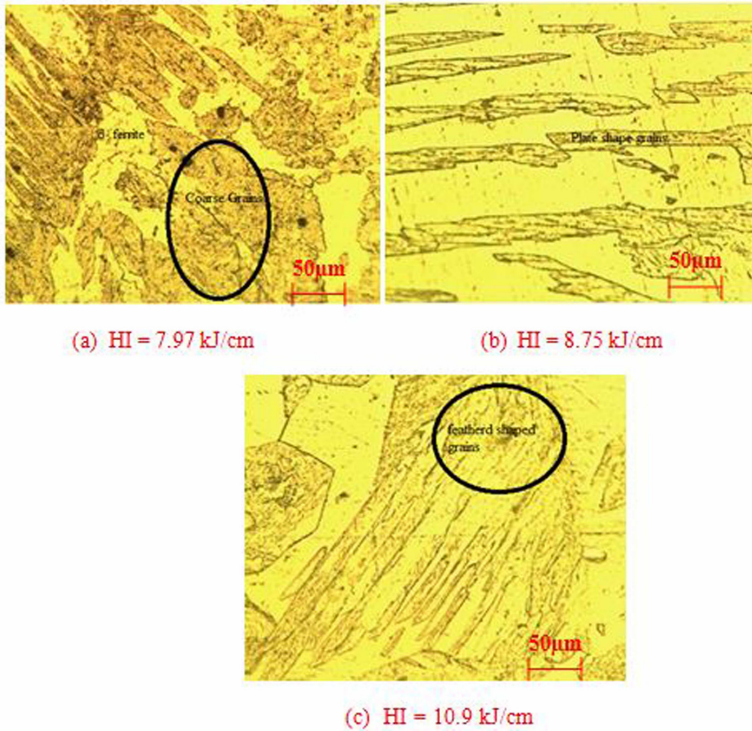


Figure 3. (a-c) The microstructure of GTA weld deposits under different heat input

the area where all phase transformations occur in the solid state which is very much required to study the microstructure of this region under different heat input. Typical change in microstructure of HAZ near to fusion line under different heat inputs of GTA weld deposits are shown in Figure 4 (a-c).

It is observed that grain coarsening near the fusion line enhanced with an increase in heat input. In general, the microstructure of HAZ contained elongated bright phase of banded delta ferrite in a matrix of martensite irrespective of change in heat input. However, it is also noticed that the ferrite content decreased as heat input got increased. The microstructure of HAZ primarily depends on the weld thermal cycle dictated by the welding process. It is well known that at higher heat input, the HAZ experiences relatively high thermal impact than low heat input. Because of higher thermal impact, the cooling rate in HAZ got

reduced and accordingly influenced the microstructure of HAZ. In addition, slow cooling rate enlarged the austenite formation and allowed ferrite dissolution in the HAZ. Similar observation was reported by Carrouge et al.,<sup>20</sup> in case of SMSS weldments under simulated conditions. In order to detect various phases present in the weldment, X-ray diffraction(XRD) studies were carried on welds obtained for different heat inputs. X-ray diffraction was carried out on planar surfaces of these weld fusion zones. Rigaku Ultimate 3 (Japan)X-ray diffractometer with CuK $\alpha$  radiation of wavelength 1.544 $\text{\AA}$  was used. Figure 5 (a-c) shows the results of X- ray diffraction patterns for weld samples under different heat inputs.

From the Figure 5 (a-c), it is seen that the peaks indicated the presence of ferrite and martensite and this XRD pattern also confirmed the constituents of weld microstructure (Figure 3 (a-c)). X-ray diffraction did not reveal the presence

of austenite in the weld samples which reflected the absence or very low volume fraction of austenite. If post weld heat treatment (PWHT) is performed at slightly above 590°C temperatures, the enriched austenite phase will be stable at room temperature<sup>21,22</sup>. If PWHT is carried out at well above 590°C temperatures, the austenite formed during PWHT will be transformed to fresh martensite during cooling<sup>21</sup>. If PWHT is carried out below 590°C temperature, the austenite content will decrease and also get transformed to fresh martensite on cooling to room temperature.

### 3.3 Mechanical properties

Effect of heat input on microhardness of weld and HAZ is given in Table 4.

There was no observable difference for the different heat inputs. However, because of lower delta ferrite content of HAZ, at high heat input the weldments showed slightly higher hardness than those of the low heat input weldments. Tensile properties of weld joints prepared under different heat inputs at different temperatures are given in Table 5.

It is observed that the tensile strength decreased with an increase in heat input irrespective of change in temperature. However, it is further observed that at a given heat input increase of temperature reduced tensile strength of the weld joints. The variation in tensile strength was primarily due to change in microstructure as explained earlier. Typical fractographs of the tensile tested samples under different heat input and temperatures are shown in Figure 6.

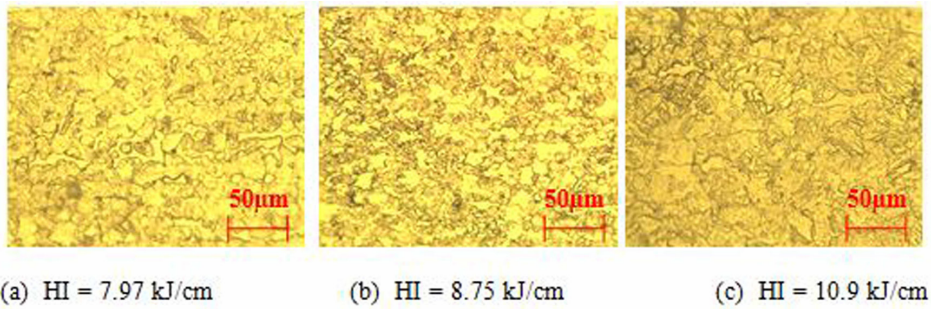


Figure 4. (a-c) The microstructure of HAZ near to fusion line under different heat input

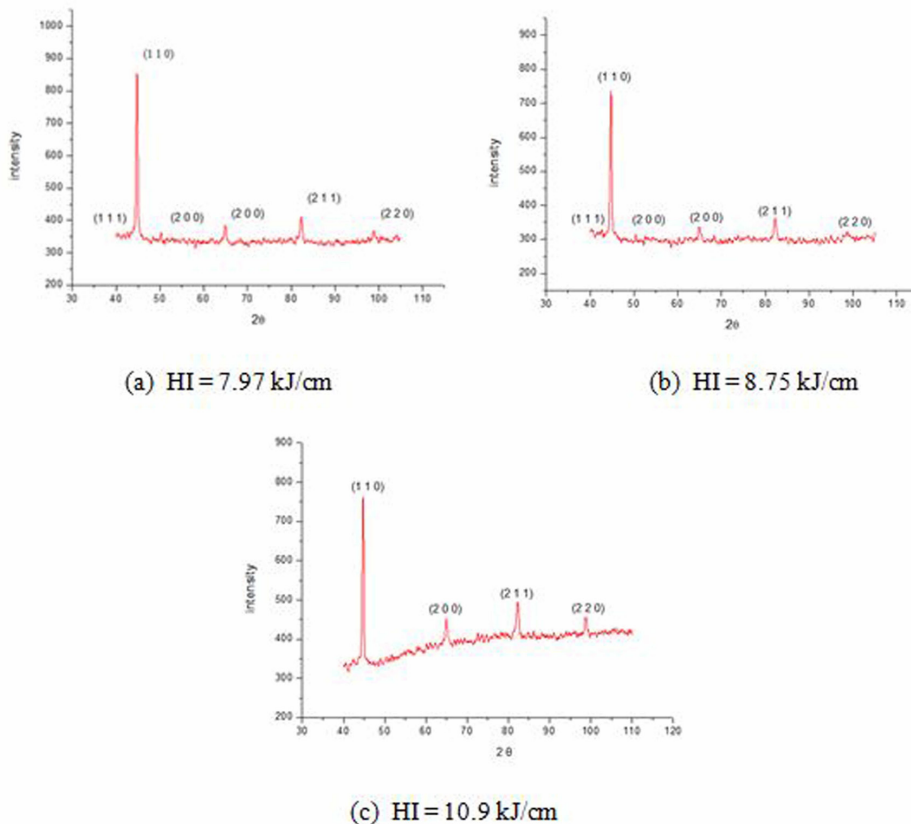


Figure 5. (a-c) XRD patterns of weld deposit under different heat input

**Table 4.** Microhardness of base metal, weld and HAZ

Exp. No.	Heat Input, kJ/cm	Microhardness of weld joint, VHN		
		Base metal	Weld	HAZ
Butt joint-1	7.97	283±5	271±4	282±4
Butt joint-2	8.75	281±4	279±3	289±3
Butt joint-3	10.9	286±4	284±6	294±5

**Table 5.** Tensile properties and impact toughness of GTA weld joints

Exp. No.	Heat Input, kJ/cm	Ultimate Tensile Strength Under Different Temperature, MPa				Impact Toughness, Joules
		RT, °C	600°C	700°C	800°C	
Butt joint-1	7.97	518	465	365	190	141
Butt joint-2	8.75	517	453	347	160	148
Butt joint-3	10.9	497	424	320	110	164
Base metal	----	516	----	----	----	175

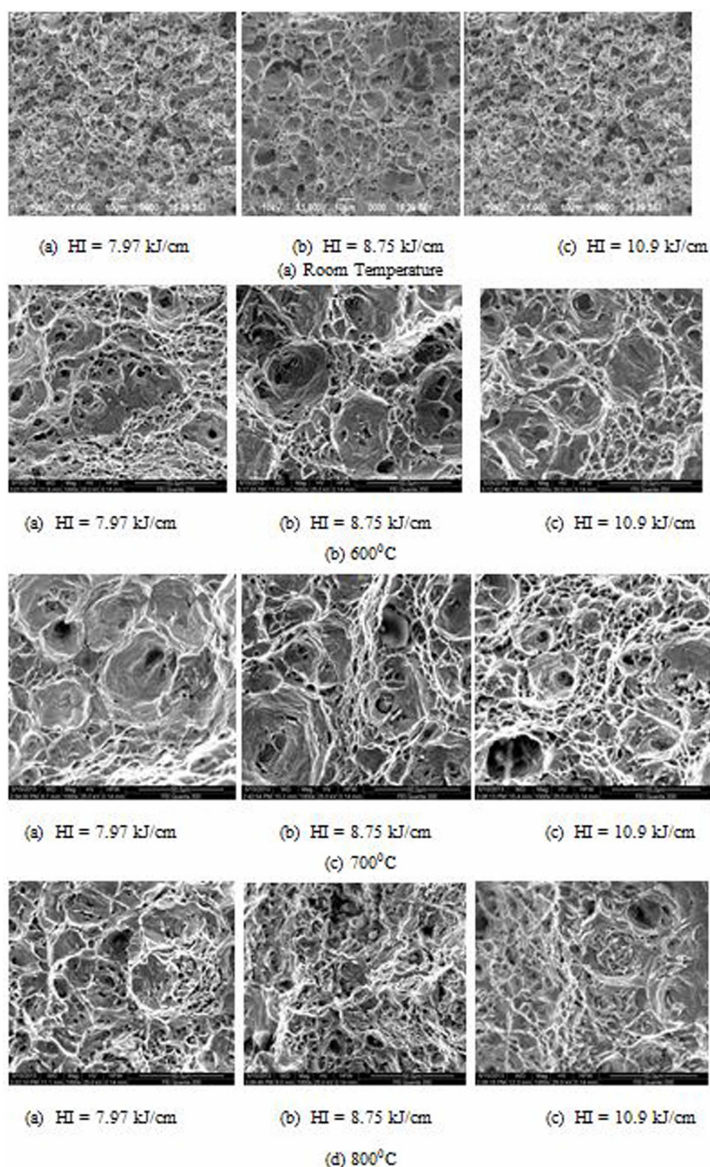


**Figure 6.** Fractographs of tensile samples under temperature as (a) RT, (b) 600°C, (c) 700°C and (d) 800°C under different heat input

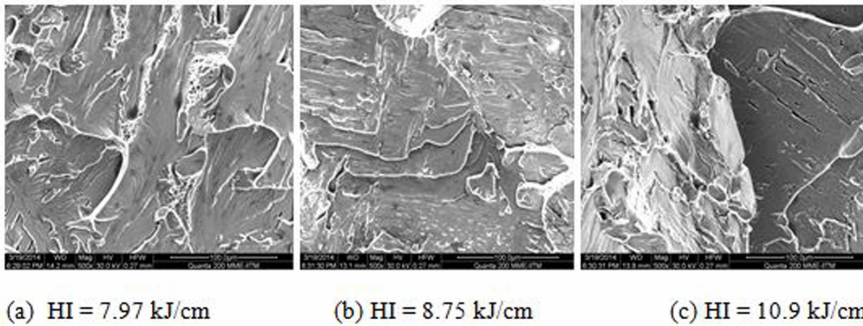


**Figure 7.** Fractographs of impact tested surface of weld deposit under different heat inputs

The fracture surface appeared as mixed mode, irrespective of heat input and temperature. Further, it is observed that, due to presence of higher delta ferrite content at high heat input weld deposit, the fracture surface showed relatively less amount of dimples than those of low heat input weld deposits. The presence of relatively high volume fraction of dimples at low heat input than high heat input plays a major role in improving the strength of the weld joint. Charpy V impact toughness of the weld produced by GTAW process under different heat inputs are also given in Table 4. It is observed that the toughness of the entire weld joints were meeting approximately 80% of the base metal toughness. In addition, an increase in heat input increased the toughness due to increased delta ferrite content. This behaviour was clearly visible as quasi-cleavage mode of fracture and it is shown in Figure 7.

#### 4. CONCLUSIONS

Effect of heat input on mechanical and metallurgical properties of AISI:410S lean super martensitic stainless steel weld joint by GTAW process was investigated. Based on the results, the following conclusions are made.

- In all cases, the microstructure of weld deposits consisted of mixture of bright phase of  $\delta$ - ferrite in the martensitic matrix. However, with an increase in heat input, the shape of the  $\delta$ - ferrite was of feathery nature.
- The amount of the  $\delta$ - ferrite content in the weld deposit increased with increasing heat input.
- Heat input had greater influence on the tensile strength and it is observed that tensile strength reduced with an increase in heat input and testing temperatures.
- Toughness of the weld joints was meeting the 80% of base metal toughness. There was an increase in toughness of welds with an increase in heat input due to an increase in delta ferrite content.
- It is recommended to select parameters which would result in optimum  $\delta$ - ferrite content in the weld as it influences the mechanical properties of the weld.

#### 5. REFERENCES

1. Farrar JC, Marshall AW. *Supermartensitic stainless steel — overview and weldability*. In: International Institute of Welding. Doc No. IX-H. 1998;1–3:423-498.
2. Lippold JC, Kotecki DJ. *Welding metallurgy and weldability of stainless steels*. Hoboken, NJ: John Wiley & Sons; 2005.
3. Karlsson L, Bruins W, Gillenius C, Rigdal S, Goldschmitz M. Matching composition supermartensitic stainless steel welding consumables. In: *9<sup>th</sup> Supermartensitic Stainless Steels*. Brussels, Belgium; 1999.
4. Ma XP, Wang LJ, Qin B, Liu CM, Subramanian SV. Effect of N on microstructure and mechanical properties of 16Cr5Ni1Mo martensitic stainless steel. *Materials and Design*. 2012; 34:74–81. DOI: 10.1016/j.matdes.2011.07.064
5. Liu YR, Ye D, Yong QL, Su J, Zhao KY, Jing W. Effect of heat treatment on microstructure and property of Cr 13 super martensitic stainless steel. *Journal of Iron and Steel Research International*. 2011;18(11):60-66. doi:10.1016/S1006-706X(11)60118-0
6. Akselsen OM, Rorvik G, Kvaale PE, Van der Eijk C. Microstructure property relationships in HAZ of new 13% Cr martensitic stainless steel. *Welding Journal*. 2004; 83(5):160–167.
7. Kumar S, Chaudhari G.P, Nath SK, Basu B. Effect of preheat temperature on weldability of martensitic stainless steel. *Materials and Manufacturing Processes*. 2012; 27(12):1382–1386. DOI :10.1080/10426914.2012.700150
8. Zappa S, Svoboda HG, Ramini de Rissone NM, Surian ES, De Vedia A. Improving supermartensitic stainless steel weld metal toughness. *Welding Journal*. 2012;91:83s-90s.
9. Omura T, Kushida T, Hayashi T, Matsuhiro Y, Komizo Y. Super 13 Cr martensitic stainless steel line pipe by super laser welding. In: *Proceedings of the Supermartensitic Stainless Steels*; 1999 May 27-28; Brussels, Belgium: Belgian Welding Institute. p. 127–133.
10. Taban E, Dhooge A, Kaluç E. Plasma Arc Welding of Modified 12%Cr Stainless Steel. *Materials and Manufacturing Processes*. 2009;24:649–656. DOI: 10.1080/10426910902769152
11. Aquino JM, Della Rovere CA, Kuri SE. Localized corrosion susceptibility of supermartensitic stainless steel in welded joints. *Corrosion Science*. 2008;64(1):35–39. doi: 10.5006/1.3278459
12. Aquino JM, Della Rovere CA, Kuri SE. Intergranular corrosion susceptibility in supermartensitic stainless steel weldments.

- Corrosion Science*. 2009;51(10):2316–2323. doi:10.1016/j.corsci.2009.06.009
13. Della Rovere CA, Ribeiro CR, Silva R, Baroni LF, Alcântara N, Kuri SE. Microstructural and mechanical characterization of radial friction welded supermartensitic stainless steel joints. *Materials Science and Engineering A*. 2013;586:86–92. doi:10.1016/j.msea.2013.08.014
  14. Della Rovere CA, Ribeiro CR, Silva R, Alcântara NG, Kuri SE. Local mechanical properties of radial friction welded supermartensitic stainless steel pipes. *Materials and Design*. 2014;56:423–427. doi:10.1016/j.matdes.2013.11.020
  15. Bala Srinivasan P, Sharkawy S.W, Dietzel W. Environmental cracking behavior of submerged arc-welded supermartensitic stainless steel weldments. *Journal of Materials Engineering and Performance*. 2004;13(2):232-236. DOI: 10.1361/10599490418433
  16. Kondo K, Ueda M, Ogawa K, Amaya H, Hirata H, Takabe H. Alloy design of super 13 Cr martensitic stainless steel (development of super 13 Cr martensitic stainless steel for line pipe-1). In: *Proceedings of the Supermartensitic Stainless Steels*; 1999 May 27-28; Brussels, Belgium: Belgian Welding Institute. p. 11-19.
  17. Van Gestel WM. Girth Weld Failures in 13Cr sweet wet gas flow lines. In: *Proceeding of the Corrosion Conference*; 2004; New Orleans, USA.
  18. Woollin P. Post weld heat treatment to avoid intergranular stress corrosion cracking of supermartensitic stainless steels. *Welding in the World*. 2007;51:31–40.
  19. Zou De-ning, Han Y, Zhang W, Fang XD. Influence of tempering process on mechanical properties of 00Cr13Ni4Mo super martensitic stainless steel. *Journal of Iron and Steel Research International*. 2010;17(8):50-54. DOI: 10.1016/s1006-706x(10)60128-8
  20. Carrouge D, Bhadeshia HK, Woollin P. Effect of  $\delta$ -ferrite on impact properties of supermartensitic stainless steel heat affected zones. *Science and Technology of Welding and Joining*. 2004; 9(5):377-389. DOI:10.1179/136217104225021823
  21. Gooch TG, Wolling P, Haynes AG. Welding metallurgy of low carbon 13% chromium martensitic steels. In: *Proceedings of the Supermartensitic Stainless Steels*; 1999 May 27-28; Brussels, Belgium: Belgian Welding Institute. p. 11-19.
  22. Folkhard H. *Welding metallurgy of stainless steels*. New York; Springer-Verlag Wien; 1988.